Lawrence Berkeley National Laboratory
Recent Work

Title

A Multiple Objective Magnet Sorting Algorithm for the ALS Insertion Devices

Permalink

https://escholarship.org/uc/item/97j155nh

Authors

Humphries, D.
Goetz, F.
Kownacki, P.
et al.

Publication Date

1994-07-01

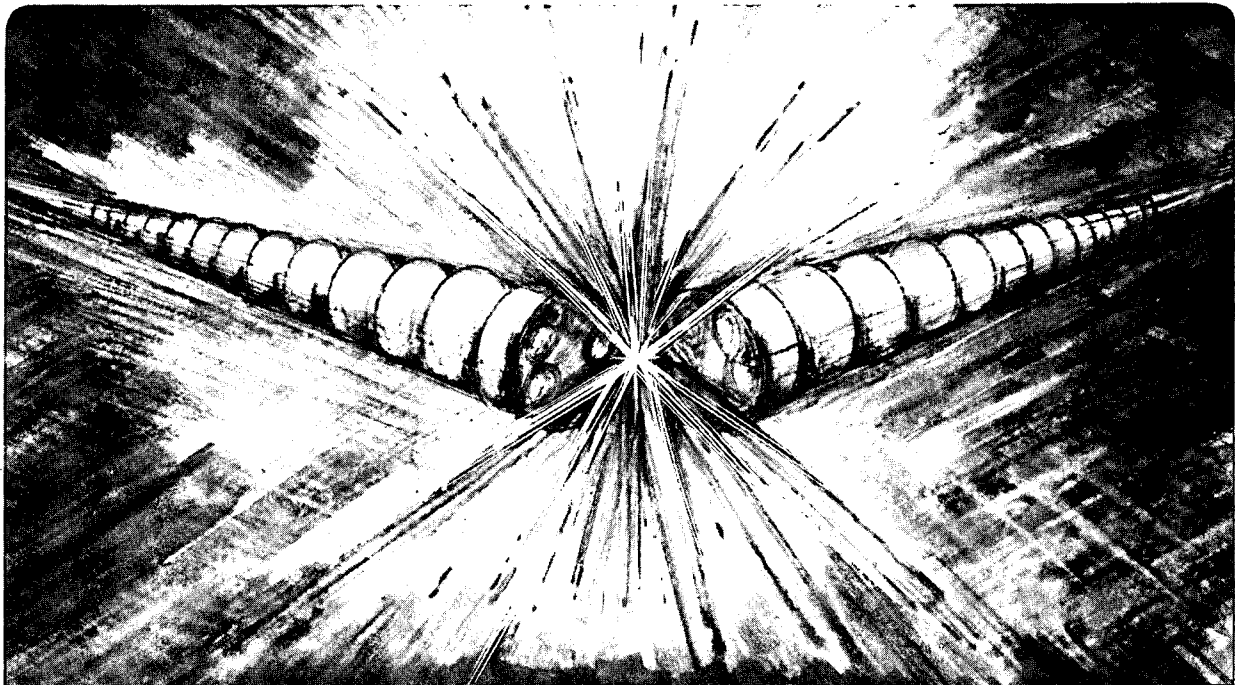# Lawrence Berkeley Laboratory

UNIVERSITY OF CALIFORNIA

Accelerator & Fusion Research Division

A Multiple Objective Magnet Sorting Algorithm for the ALS Insertion Devices

D. Humphries, F. Goetz, P. Kownacki, S. Marks, and R. Schlueter

July 1994

DISCLAIMER

A MULTIPLE OBJECTIVE MAGNET SORTING ALGORITHM FOR THE ALS INSERTION DEVICES*

D. Humphries, F. Goetz, P. Kownacki, S. Marks, and R. Schlueter

Advanced Light Source
Accelerator and Fusion Research Division
Lawrence Berkeley Laboratory
University of California
Berkeley, CA 94720

July 1994

A Multiple Objective Magnet Sorting Algorithm for the Advanced Light Source Insertion Devices*

D. Humphries, F. Goetz, P. Kownacki, S. Marks, and R. Schlueter

Advanced Light Source, Lawrence Berkeley Laboratory, University of California, Berkeley, California 94720

Abstract

Insertion devices for the Advanced Light Source (ALS) incorporate large numbers of permanent magnets which have a variety of magnetization orientation errors. These orientation errors can produce field errors which affect both the spectral brightness of the insertion devices and the storage ring electron beam dynamics. A perturbation study was carried out to quantify the effects of orientation errors acting in a hybrid magnetic structure. The results of this study were used to develop a multiple stage sorting algorithm which minimizes undesirable integrated field errors and essentially eliminates pole excitation errors. When applied to a measured magnet population for an existing insertion device, an order of magnitude reduction in integrated field errors was achieved while maintaining near zero pole excitation errors.

I. Introduction

A partial lower magnetic structure for an ALS undulator is shown Fig. 1. It is a hybrid structure consisting of ferromagnetic poles which are excited by permanent magnets. The principal magnetization orientation of the permanent magnets is parallel to the electron beam or z axis of the coordinate system shown in the figure.

In order to maintain the spectral quality of the light produced by the insertion devices, the poles of the device must be uniformly excited by the permanent magnets. Non-iterative algorithms have been previously developed and successfully applied to magnet populations to achieve uniform pole excitation[1]. These algorithms primarily order and arrange magnets using the principal component of the magnetic moment M_z. All three components, M_x, M_y and M_z are obtained by Helmholz coil measurement[2].

Experience with the first ALS undulators[3] has shown that the minor components of the magnetic moments, M_x and M_y, may combine in the overall magnetic structure of a given insertion device to result in a non-uniform transverse distribution of perturbing fields that may adversely affect electron beam dynamics. These error fields are typically large enough to require external correction[4] to prevent degradation of beam lifetime and beam dynamics effects.

The perturbation study described here uses the results of the first stage algorithm for uniform pole excitation as its starting point. Effects of particular magnetization minor components acting in a known hybrid magnetic structure, the ALS U5.0, were quantified and an iterative algorithm was developed which acts on a limited parameter space to minimize localized perturbation fields and their integrals.

II. Perturbation Modeling

In order to determine the effects of a given minor component, the model shown in Fig. 2 was constructed and solved using the 3D magnet code AMPERES[5]. The model is comprised of four poles above the midplane and four below with a single permanent magnet between the second and third upper poles. Four cases were modeled consisting of two transverse magnet positions with a vertical and horizontal orientation for each position. Normal and skew fields (B_y and B_x) were calculated on the midplane between the two pole arrays for each case. The objective of the magnet positioning was to model the effects of the three magnets in each six-magnet-array that are closest to the midplane and thus closest to the electron beam. The three magnets in the back row of each array are ignored because of their negligible direct field effect on the midplane.

The fields were calculated for a center magnet and the adjacent magnet in the positive x direction which by appropriate symmetry yields the fields for the magnet on the negative x side of the center magnet. The fields for the corresponding three magnets below the midplane

are obtained by simple symmetry transforms of the fields from the three magnets above the midplane.

Thus we calculate B_x and B_y field distributions from two magnet orientations and two magnet positions which results in eight fundamental perturbation fields. One of these perturbation fields in shown in the graph of Fig. 3. To completely describe the total perturbation field for a combination of three magnets above the midplane and three below the midplane, we must superimpose twelve perturbation fields each for the final normal and skew fields. These twenty-four field distributions are derived directly from the eight fundamental perturbation fields in the manner described above.

III. Statistical Study

Before beginning this optimization effort, it was necessary to confirm that the magnet minor components were the primary source of observed integrated field errors in the first ALS insertion devices. Towards this end, a statistical study was devised which took into account the average values and rms variations of minor components for magnets positioned over the electron beam and those to the right and left of the center magnets. Because of the alternating polarity of the insertion device poles, the sign of systematic horizontal minor components alternates as well which implies that they should cancel. Thus only vertical minor components produce a systematic effect. To quantify non-systematic effects, the rms variations of both horizontal and vertical components were used to calculate the standard deviation of expected values.

Average vertical minor component values were assigned to three magnets above and below the midplane. Perturbation fields from the models described in section II above were calculated for the magnets and multiplied by the number of upper and lower pole pairs that were measured in the comparison insertion device. When the results were compared to the measured integrated error fields there was both qualitative and quantitative agreement to within approximately twenty percent. The clear conclusion of this study is that most of the residual field errors measured in the periodic section of these insertion devices are a direct result of magnetization orientation errors in the permanent magnets which power the structures.

IV. Calculation of Perturbation Fields

The perturbation fields for the entire midplane of the comparison insertion device were next calculated using the known distribution of measured minor components. The normal and skew perturbation fields for each magnet facing the midplane were calculated for both horizontal and vertical minor components. These fields were then superposed to form the entire skew and normal perturbation fields. They were then integrated as a function of z and compared to the measured, integrated fields for the device. Fig. 4 shows the normal field comparison while Fig. 5 gives the comparison of skew fields. As expected, these results show

closer agreement with measured results than that of the statistical comparison described above.

V. Optimization Parameter Space

A consequence of the first stage algorithm that achieves uniform pole excitation is that arrays of six magnets for each pole are established. The magnets in these arrays cannot be recombined with magnets from other arrays in the structure without jeopardizing their uniform M_z averages. This condition limits the number of free parameters for minimizing other error effects. For minimization of minor component effects there are four available parameters: magnet positioning, magnet rotation, single pole rearrangement and pole pair rearrangement.

In each six magnet array, the three magnets closest to the midplane may assume any of six position permutations with no violation of pole excitation conditions. Similarly there are eight magnet rotation permutations for a 180 degree rotation of these three magnets and many more permutations for square magnets that may be rotated in 90 degree increments.

Single magnet arrays associated with a pole may be exchanged with any other array in the device, and pole pairs may also be exchanged without affecting pole excitation.

The first three parameters affect both integrated field errors in the device and local errors. Localized error field distributions perturb beam trajectories within the length of the insertion device and may result in undesirable integrated error fields for electron trajectories which are not parallel to the central beam trajectory.

The fourth parameter is the positioning of upper and lower pole pairs in the device. This parameter has no effect on net integrated fields but can affect first and second integrals and thus beam trajectories within the device. Pole pair rearrangement is logically exercised after optimization using the previous parameters. It has no effect on prior optimization for uniform pole excitation nor on the optimized condition resulting from the application of the other three previously described parameters.

For the current effort, the first two parameters were applied to a second stage optimization and the fourth parameter was applied to a third stage optimization of the test magnetic structure. Application of the third parameter, single pole recombination, was left for further study since it results in significant lengthening of optimization time.

VI. Objective Functions for Optimization

Two objective functions were developed, $F(\bar{B}_p)$ and $G(\bar{B}_p)$ where $\bar{B}_p$ is the general, midplane perturbation field of the device. The first was used for optimizing with the first two parameters, magnet positioning and rotation, while the second was used for the independent fourth parameter, pole pair rearrangement.

The first objective function, $F(\bar{B}_p)$, is composed of four components as follows:

$$F(\bar{B}_p) = m_1 f_1(B_{ps}) + m_2 f_2(B_{pn}) + m_3 f_3(B_{ps}) + m_4 f_4(B_{pn}) \qquad (1)$$

where f_1 and f_2 are the Euclidean norms of the integrated skew and normal perturbation fields respectively. This is equivalent to the rms of the integrated perturbation fields up to a multiplicative constant.

The f_3 and f_4 components represent the Euclidean norms of the entire localized skew and normal perturbation field distributions. Specifically, this is the square root of the sums in x and in z of the squared field distributions of individual up-down pole pairs. The m_1 through m_4 are weight variables used to control the emphasis of the optimization. B_{ps} and B_{pn} represent skew and normal perturbation fields. For all f_i, Gaussian weight functions are applied to the transverse field distributions for each pole pair to improve the optimization near the electron beam trajectory.

The f_1 and f_2 objective functions describe integrated field effects while the f_3 and f_4 objective functions reflect localized perturbation magnitudes which affect particle trajectories within the length of the insertion device.

The second objective function, $G(\bar{B}_p)$, is a weighted sum of rms trajectory deviations and is the criterion for optimization using the fourth parameter which is the ordering of pole pairs. The non-normalized function is given by

$$G(\bar{B}_p) = w_1 \sum_x w_3(x) \left\| \iint B_{pn} dz^2 \right\|_2 + w_2 \sum_x w_4(x) \left\| \iint B_{ps} dz^2 \right\|_2 \qquad (2)$$

Here w_1 and w_2 are skew and normal field weight variables, $w_3(x)$ and $w_4(x)$ are transverse weight functions and B_{pn} and B_{ps} represent the normal and skew perturbation fields as before. The normed double integral is used to indicate the Euclidean norm or rms value, up to a multiplicative constant, of the beam trajectory deviations.

The normalized function is given by $\tilde{G}(\bar{B}_p) = G(\bar{B}_p)/G_0(\bar{B}_p)$ where $G_0(\bar{B}_p)$ is the condition of the device at the start of this third stage of optimization.

VII. Optimization Results

After systematic and iterative second stage optimization using the first two parameters (magnet inversion and position permutations), the magnitude of the first objective function, $F(\bar{B}_p)$, was reduced by approximately 75%. This reflects a 50% reduction in rms field errors and a 99% reduction in integrated field errors. As indicated in Figs. 6 and 7, dramatic reductions in integrated normal and skew perturbation fields were achieved.

Results from the third stage optimization using the fourth parameter (permutations of pole pair locations), show that the magnitude of the second objective function, $\tilde{G}(\bar{B}_p)$, which is a measure of rms trajectory deviations, was reduced by approximately 40%. Actual calculated

trajectory magnitudes within a +/- 2 cm beam aperture were reduced by 85% for both horizontal and vertical trajectories.

In summary, these results indicate that the second and third stages of this algorithm are capable of near elimination of integrated error fields caused by magnet orientation errors and significant reduction of trajectory deviations within the insertion device. This is accomplished with no degradation of the uniform pole excitation condition achieved by the first stage sorting algorithm.

Acknowledgment

1) D. Humphries, E. Hoyer, B. Kincaid, S. Marks, and R. Schlueter, *Proceedings of the 13th International Conference on Magnet Technology*, Victoria, British Columbia, Canada, September, 1993, LBL-34644.

2) S. Marks, J. Carrieri, C. Cook, W. Hassenzahl, E. Hoyer, and D. Plate, *Proceedings of the 1993 IEEE Particle Accelerator Conference* , Washington, DC, May, 1993.

3) E. Hoyer, S. Marks, P. Pipersky, R. Schlueter, SRI'94, July, 1994.

4) E. Hoyer, J. Akre, J. Chin, W. Gath, W.V. Hassenzahl, D. Humphries, B. Kincaid, S. Marks, P. Pipersky, D. Plate, G. Portmann, R. Schlueter, SRI'94, July, 1994.

5) AMPERES Three-Dimensional Magnetic Field Solver, <u>Users and Technical Manual</u>, Integrated Engineering Software Inc., Winnipeg, Manitoba, Canada, 1991.

Nd-Fe-B Permanent Magnets

Vanadium Permendur Poles
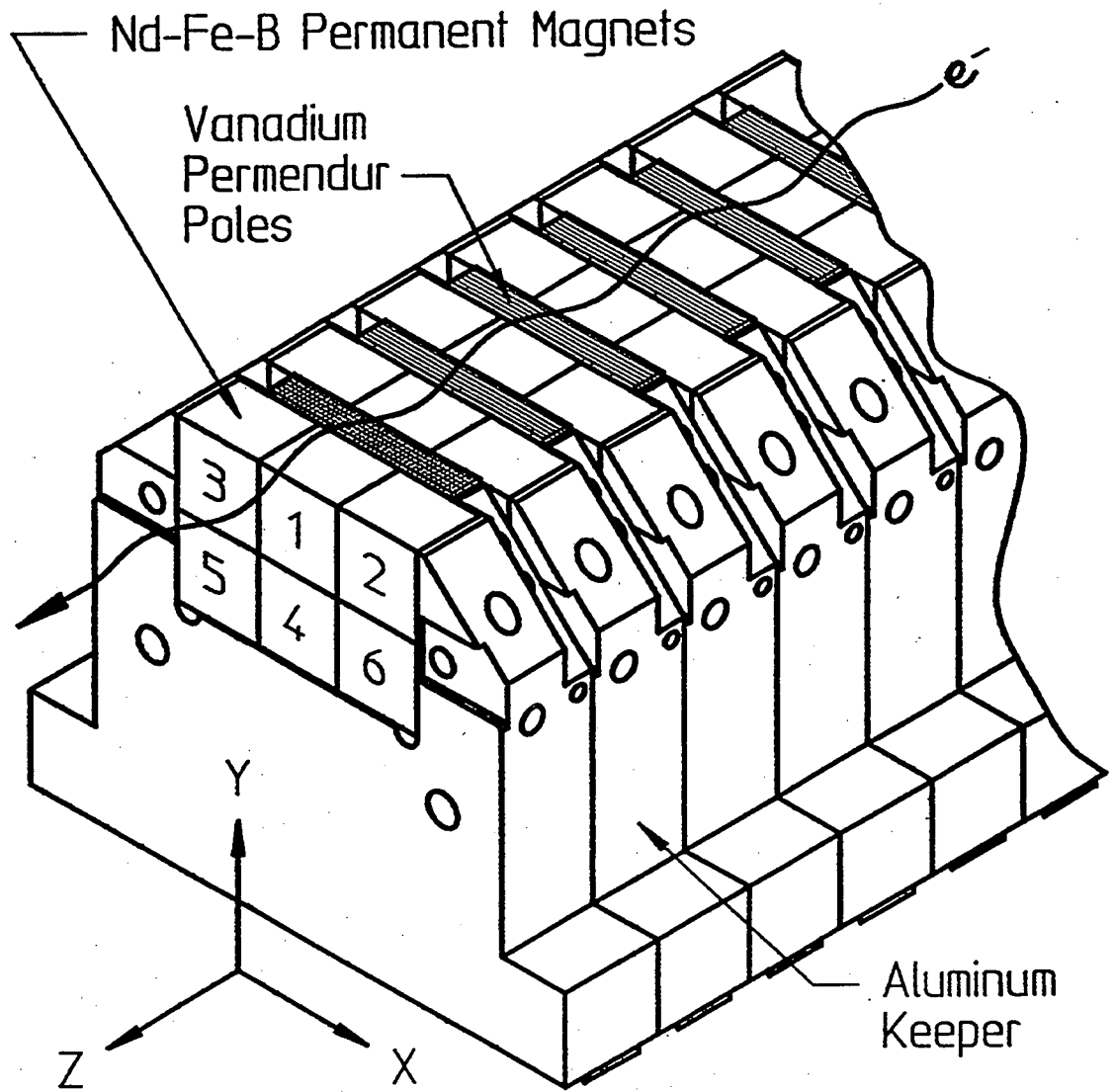
e^-

Aluminum Keeper

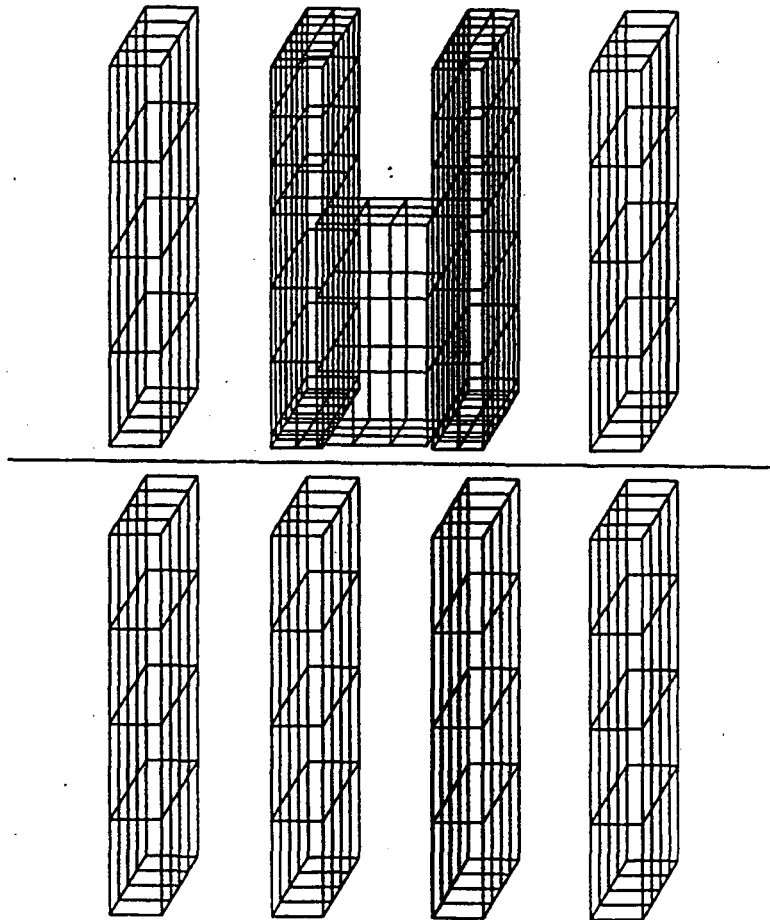Fig. 1 Section of insertion device lower magnetic structure.

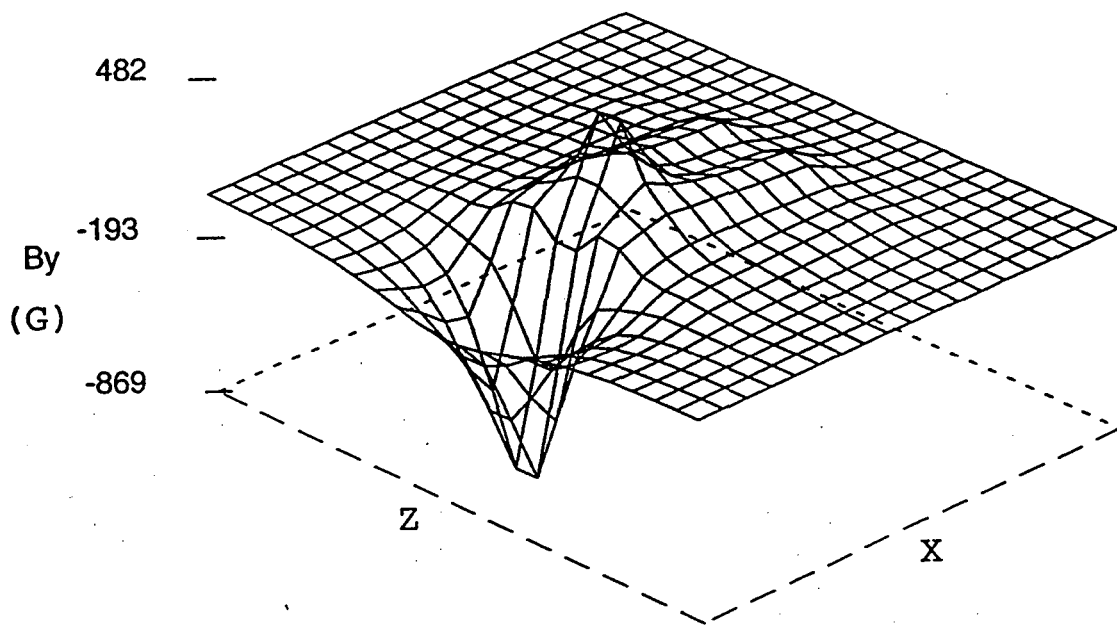Fig. 2 Typical eight pole 3D model with permanent magnet between upper poles for perturbation calculations.

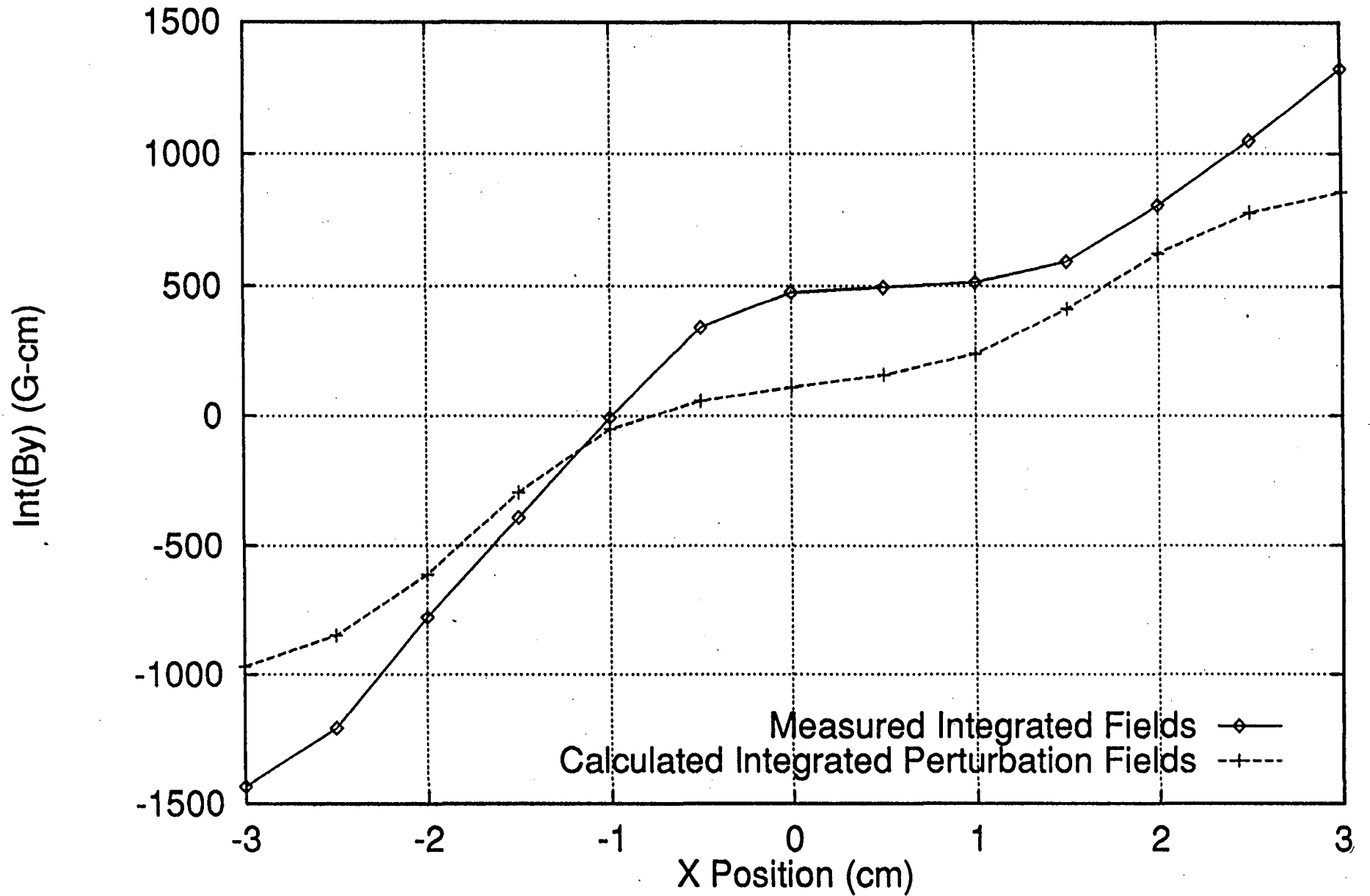Fig. 3 Example of fundamental perturbation field for horizontal minor component.

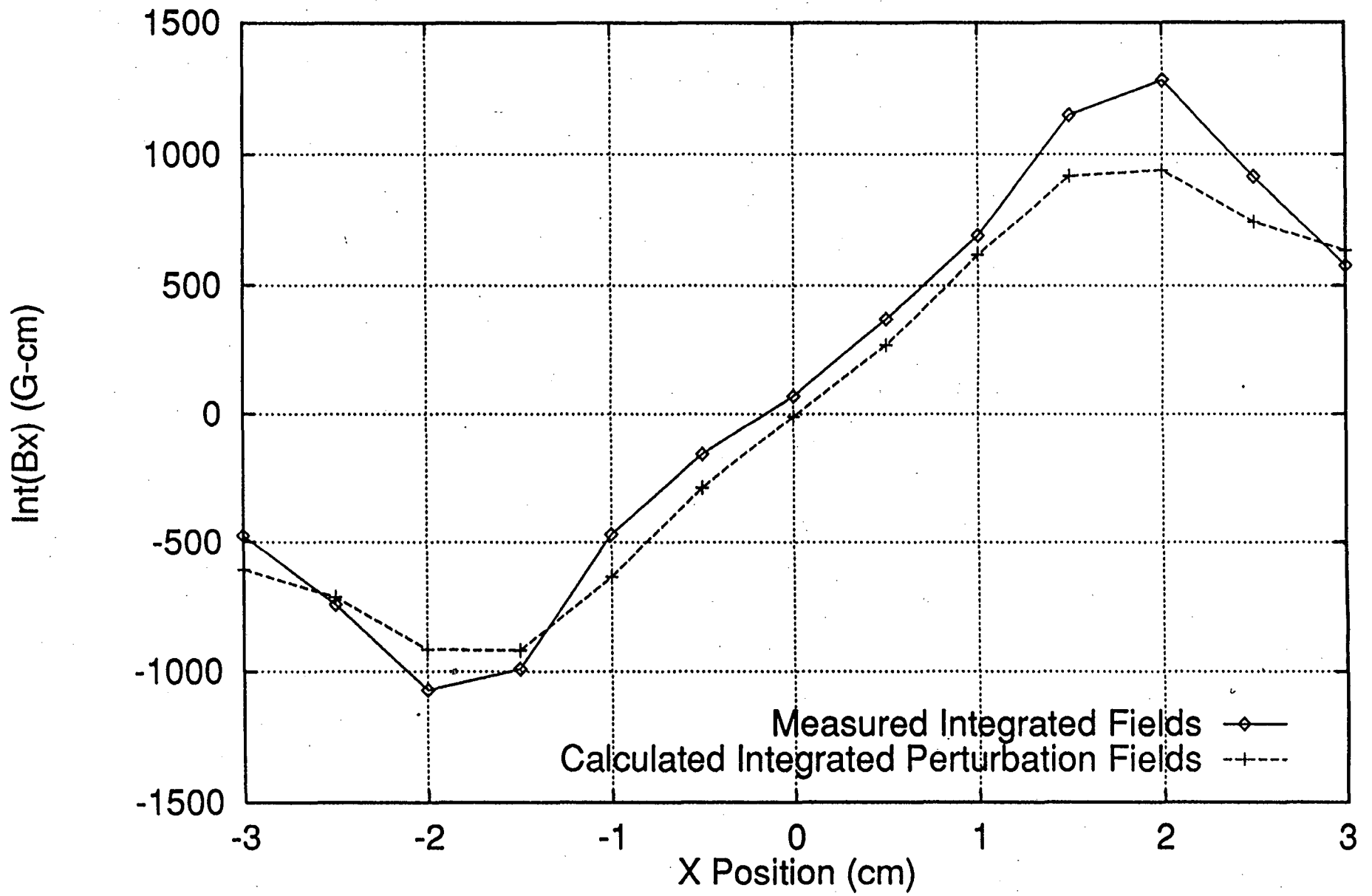Fig. 4 Measured vs calculated integrated normal fields
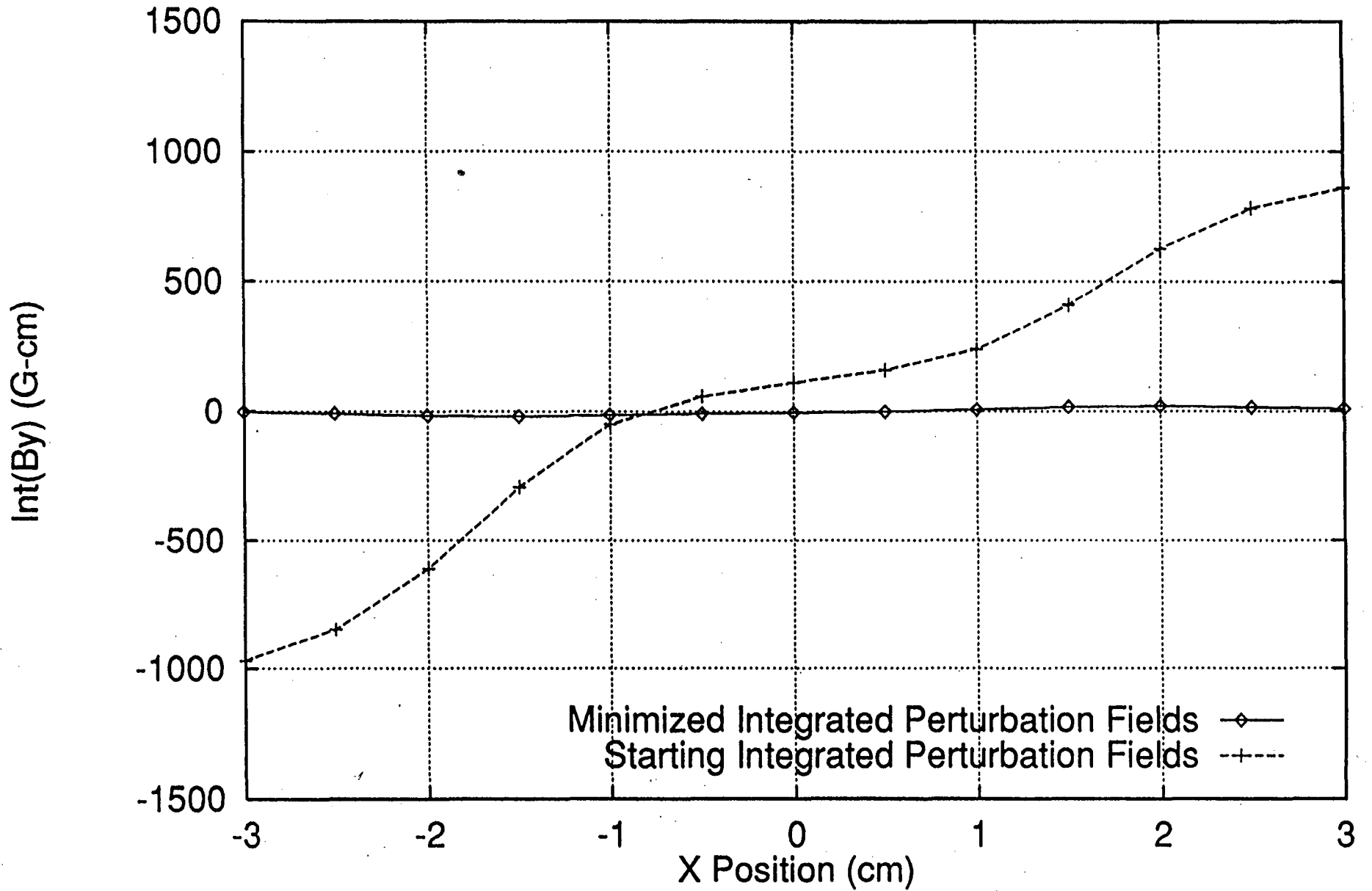
Fig. 5 Measured vs calculated integrated skew fields

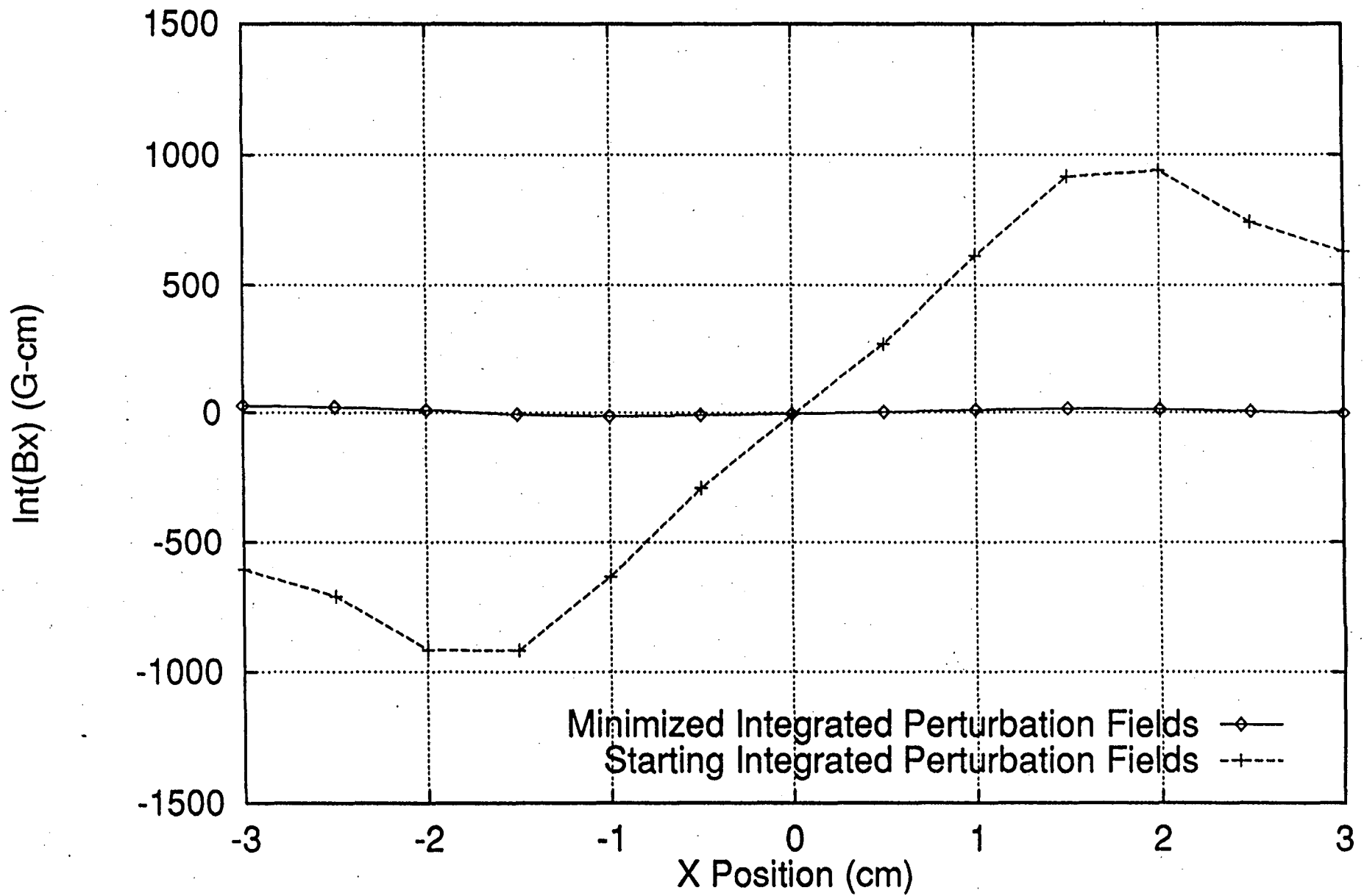Fig. 6 Optimized, integrated normal perturbation fields vs original calculated fields

Fig. 7 Optimized, integrated skew perturbation fields vs original calculated fields